To What Extent Can UAV Photogrammetry Replicate UAV LiDAR to Determine Forest Structure? A Test in Two Contrasting Tropical Forests

Iain M. McNicol[1] , Edward T. A. Mitchard[1] , Chiara Aquino[1] , Andrew Burt[2], Harry Carstairs[1], Creck Dassi[3] , Anaick Modinga Dikongo[3] , and Mathias I. Disney[2,4]

[1]School of GeoSciences, University of Edinburgh, Edinburgh, UK, [2]Department of Geography, UCL, London, UK, [3]Agence Gabonais d'Etudes et d'Observations Spatiales (AGEOS), Libreville, Gabon, [4]Department of Geography, NERC NCEO-UCL, London, UK

Abstract Tropical forests are complex multi-layered systems, with the height and three-dimensional (3D) structure of trees influencing the carbon and biodiversity they contain. Fine-resolution 3D data on forest structure can be collected reliably with Light Detection and Ranging (LiDAR) sensors mounted on aircraft or Unoccupied Aerial Vehicles (UAVs), however, they remain expensive to collect and process. Structure-from-Motion (SfM) Digital Aerial Photogrammetry (SfM-DAP), which relies on photographs taken of the same area from multiple angles, is a lower-cost alternative to LiDAR for generating 3D data on forest structure. Here, we evaluate how SfM-DAP compares to LiDAR data acquired concurrently using a fixed-wing UAV, over two contrasting tropical forests in Gabon and Peru. We show that SfM-DAP data cannot be used in isolation to measure key aspects of forest structure, including canopy height (%Bias: 40%–50%), fractional cover, and gap fraction, due to difficulties measuring ground elevation, even under low tree cover. However, we find even in complex forests, SfM-DAP is an effective means of measuring top-of-canopy structure, including surface heterogeneity, and is capable of producing similar measurements of vertical structure as LiDAR. Thus, in areas where ground height is known, SfM-DAP is an effective method for measuring important aspects of forest structure, including canopy height, and gaps, however, without ground data, SfM-DAP is of more limited utility. Our results support the growing evidence base pointing to photogrammetry as a viable complement, or alternative, to LiDAR, capable of providing much needed information to support the mapping and monitoring of biomass and biodiversity.

Plain Language Summary Tropical forests support a diverse array of plant and animal species, and are highly productive, playing a vital role in the global carbon cycle. Quantifying the height and density of these forests can help us better understand the amount of carbon and biodiversity they store. Generating such data over large areas is possible using Light Detecting and Ranging (LiDAR) scanners mounted on an aircraft or on Unoccupied Aerial Vehicles, although these data are expensive to collect and process. An alternative method is photogrammetry, which involves collecting several overlapping photographs of the same area from different viewpoints, from which we can generate a 3D reconstruction of the surface. This approach is much cheaper, potentially allowing us to map forests with greater frequency. However, we find this method cannot be used to measure key elements like tree height, due to difficulties seeing, and thus estimating ground elevation. The forest canopy surface can be measured fairly well while measurements of vertical structure are broadly similar to LiDAR data. If the ground height is known, then photogrammetry is a viable means of collecting important data on forest structure necessary for mapping carbon and biodiversity.

1. Introduction

Accurate and detailed measurements of forest structure are essential to improving our knowledge of a range of important ecosystem services and functions, including carbon storage, productivity, habitat quality, and biodiversity. The recent proliferation of space- and air-borne platforms incorporating light detection and ranging (LiDAR) sensors will provide new insights into these variables due to their ability to map key aspects of forest structure across large areas (10s km^2), and at fine resolutions (≤ 1 m). Forest structure can be characterized in different ways when measured from above using LiDAR, with common measurements including the horizontal distribution of vegetation across an area, such as its height, heterogeneity, fractional cover, and gap fraction, as well as

Writing – review & editing: Iain M. McNicol, Edward T. A. Mitchard, Andrew Burt, Mathias I. Disney

the vertical distribution and density of plant material below the canopy surface. Retrieving this information is important for several reasons: first, measurements of tree height and fractional cover are essential components in models that estimate aboveground biomass (AGB; Asner & Mascaro, 2014; Jucker, Asner, Dalponte, Brodrick, Christopher, et al., 2018; Knapp et al., 2020). Measurements of 3D vertical forest structure are also important for estimating AGB (Dubayah et al., 2020; Meyer et al., 2013), and for understanding habitat characteristics and biodiversity patterns on the basis that structurally complex forests provide space for species with different specializations and niches (Burns et al., 2020; Lopatin et al., 2016; Marselis et al., 2020; Schneider et al., 2020; Valbuena et al., 2020). These data are most commonly acquired using aircraft, however, high acquisition costs mean that data collection, particularly in more remote tropical forests, is typically done in an ad hoc manner, and rarely repeated (Xu et al., 2017). New space-borne LiDAR missions such as NASA's Global Ecosystem Dynamics Investigation LiDAR are helping fill these key observation gaps by providing global measurements of forest structure, including new estimates of AGB, however, coverage is sparse and collected at a coarse resolution compared to airborne platforms (separated 25 m footprints, compared to cm diameter footprints), and the data collection is time-limited (Dubayah et al., 2020).

In recent years, Unoccupied Aerial Vehicles (UAVs; Joyce et al., 2021) equipped with small, lightweight LiDAR sensors have become a viable alternative to LiDAR data collection via aircraft (Brede et al., 2019; Kellner et al., 2019; Yin & Wang, 2019). The unique combination of low flight altitudes (10s–100 m)—which normally removes the need to notify national civil aviation authorities before operation—slower flight speeds, and a wider field of view mean that UAV-borne LIDAR is capable of producing 3D point clouds with sufficient density ($100s-1,000$ pts/m^2 vs. 10s pts/m^2 for aircraft) to allow individual tree crowns, and branches to be resolved (Brede et al., 2017, 2019; Kellner et al., 2019; Puliti, Breidenbach, & Astrup, 2020). Improvements in flight times (up to 1 h) mean UAVs can now cover relatively large areas (1–10s km), and so provide an important bridge between fine-scale ground measurements, for example, from Terrestrial Laser Scanning (Burt et al., 2021; Disney et al., 2018), and sparse and/or coarse resolution satellite data, the resolution of which is often too coarse (20–50 m +) to reliably capture small-scale patterns and changes associated with growth and mortality (Assmann et al., 2020; Espírito-Santo et al., 2014). However, there remain potentially significant barriers to the widespread adoption of the technology, namely the capital cost of equipment, which includes the sensor itself, GPS-IMU hardware to accurately measure UAV position, as well as a UAV platform capable of carrying a relatively heavy payload (>3 kg), which itself may require special flights permissions, and/or trained, certified pilots to operate (Beland et al., 2019; Brede et al., 2017; Kellner et al., 2019). Platform and sensor may be subject to import/export control regulations, while widespread restrictions on transportation of powerful batteries on commercial airlines create logistical issues if the system is being applied outside the country of origin.

To that end, alternative methods based on digital aerial photogrammetry (hereafter DAP) have been posited as a potential lower-cost source of fine-resolution 3D information on forest structure (Iglhaut et al., 2019; Puliti, Dash, et al., 2020). The approach, which uses multiple images collected from different positions to construct a 3D model of the visible surface—a technique termed Structure from Motion (SfM)—can generate point cloud data similar to that obtained from LiDAR, but using hardware a tiny fraction of the cost and weight. Its application has increased markedly over the past decade (Goodbody et al., 2019), due in part to the utility of consumer-grade imaging platforms and sensors, and the associated low cost of acquiring data, but also due to increases in computing capacity, and the availability of commercial and open-source software for processing what can often run to hundreds to thousands of images (Bayley & Mogg, 2020). This, combined with the ability to generate fine resolution orthomosaic images covering a whole study area, means that image-based methods are a potentially attractive alternative to more costly LiDAR data collection.

However, as with LiDAR data, there are challenges to image-based methods that potentially limit its widespread usage, particularly over dense tropical forests. The first is that optical images, without the penetration of the laser beams of LiDAR, mostly only collect information from the canopy surface, with information on lower strata or the ground only provided in rare canopy gaps. This creates known errors when estimating important variables such as tree height, due to difficulties in extracting the ground elevation (Roşca et al., 2018; Swinfield et al., 2019; Vaglio Laurin et al., 2019). A common solution is to use LiDAR-derived ground elevations, with SfM-DAP used for repeat, or retrospective monitoring of canopy structure (Ali-Sisto & Packalen, 2017; Gobakken et al., 2015; Goodbody et al., 2019; Krause et al., 2019; St-Onge et al., 2008), although this negates many of the original attractions of using SfM-DAP over LiDAR. Second, tropical forests present a challenge for image and feature

matching algorithms that rely on visual similarities between overlapping images to reconstruct the 3D surface model. For example, trees and dense vegetation, due to their complex shape and structure may appear very different between overlapping images, which coupled with potential movement (e.g., due to wind) and areas of occlusion (i.e., obscured/shadowed areas), can potentially lead to incomplete reconstruction and/or noisy point clouds (Cunliffe et al., 2021). Differences in lighting conditions, for example, due to changing cloud cover, or the time of day the data was acquired, may also affect the consistency of image-based point clouds, which is potentially problematic when conducting missions across large areas, or conducting repeat measurements over several days.

Although the benefits and challenges of structure-from-motion (SFM) photogrammetry are well understood (Goodbody et al., 2019; Iglhaut et al., 2019)—having been widely applied for surveying over temperate forests—there remains limited data on how well it performs in tropical forests, and under what conditions it can begin to resemble information obtained by LiDAR. For example, it is unclear how the retrieval of tree height, and other metrics vary depending on local forest structure, such as canopy cover or vegetation density (Mlambo et al., 2017; Wallace et al., 2016), and whether these errors are systematic, or primarily random in nature. Understanding the nature of these errors is important, as if they can be taken into account it may be that SfM-DAP is sufficient for many use cases where LiDAR (or no data collection at all) might have been the alternative. Further, as with Li-DAR, the increasing use of UAVs provides new opportunities for SfM-DAP, given their ability to image the forest from a greater number of viewpoints, and potentially image beneath the canopy itself, reducing or removing the aforementioned challenges.

To that end, in this article, we compare various forest structural metrics relevant to AGB estimation, and to our understanding of wider ecosystem functions such as biodiversity and productivity. These data sets were generated using extensive LiDAR and SfM-DAP data collected concurrently using a UAV over two contrasting areas of tropical forest in Gabon and Peru. The scale of our data sets, which cover a larger area than previous comparisons, provides a novel basis for assessing the capacity of SfM-DAP, and where it can be successfully applied-information that is crucial in order to facilitate rapid, low-cost measurement and monitoring of tropical forests.

2. Methods

2.1. Study Region

The two study areas are located in remote areas of Peru and Gabon, selected primarily due to their contrasting vegetation structures. The Peruvian site is centered on a small community (Communidad Nativa Bélgica) located approximately 40 km west of Iñapari in the Madre de Dios region. The area has a mean annual rainfall of ~1,800–2,200 mm, with a distinct dry season between June and October. The area of interest covers approximately 20 km^2 and comprises a mosaic of agricultural land, pasture, secondary, and mature forest (Figure 1). The vegetation is dominated by species in the genus *Socratea*, *Matisia* and *Pseudolmedia*, with tree densities ranging from ~500 to 600 stems/ha (counting stems >10 cm diameter at 1.3 m). The site in Gabon is located in an active logging concession operated by Rougier Gabon, and covers 10 km^2 with the vegetation consisting almost exclusively of mature forest, with more open patches located close to the track network (Figure 1). Tree density is markedly lower, in the range of 200–300 stems/ha, with tree species composition typically dominated by slower growing species, with denser wood, including those in the genus *Coula*, *Coelocaryon*, and *Pentaclethra*. The area has a similar mean annual rainfall of 1,900–2,100 mm with a short dry season from January–February, and another between June and September.

2.2. Data Acquisition

Data were collected in July 2019 (Peru) and January 2020 (Gabon) using a DELAIR (DT26X fixed-wing UAV equipped with a RIEGL miniVUX-1DL discrete-return LiDAR sensor (RIEGL Laser Measurement Systems GmbH, Horn, Austria), and a 36 MP RGB camera. The LiDAR sensor operates in the near-infrared (905 nm), has a field of view ±23° off-nadir, and has laser beam divergence of 1.6 mrad with up to five returns from each pulse digitized. The payload also includes an Applanix APX-15 IMU and L1/L2 GNSS receiver for PPK correction of the flight trajectory (Figure 2). The RGB camera has a horizontal and vertical field of view of ±20°, and ±17° off-nadir respectively, with an acquisition rate of 1 image/s.
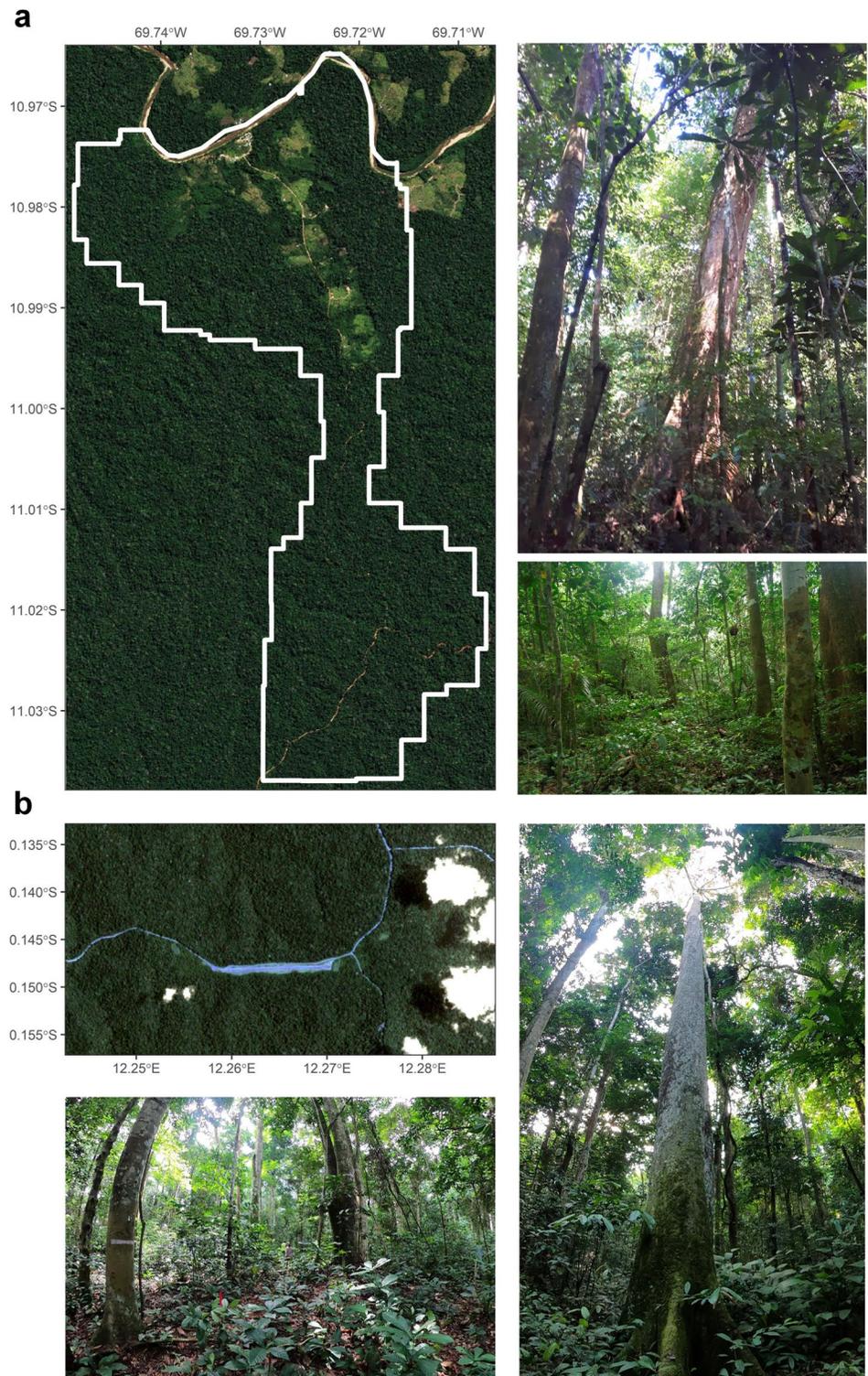
Figure 1. Location and extent of the two study areas in (a) Peru (image centered on: −11.00, −69.72) and (b) Gabon (image center: −0.1480, 12.266), with base satellite imagery from Planet Labs (RapidEye and PlanetScope respectively). For the Gabon site, the image extent is consistent with LiDAR data coverage and are presented on the same scale as the map of the Peru site. The photographs adjacent to each map give an insight to the forest structure at each site.
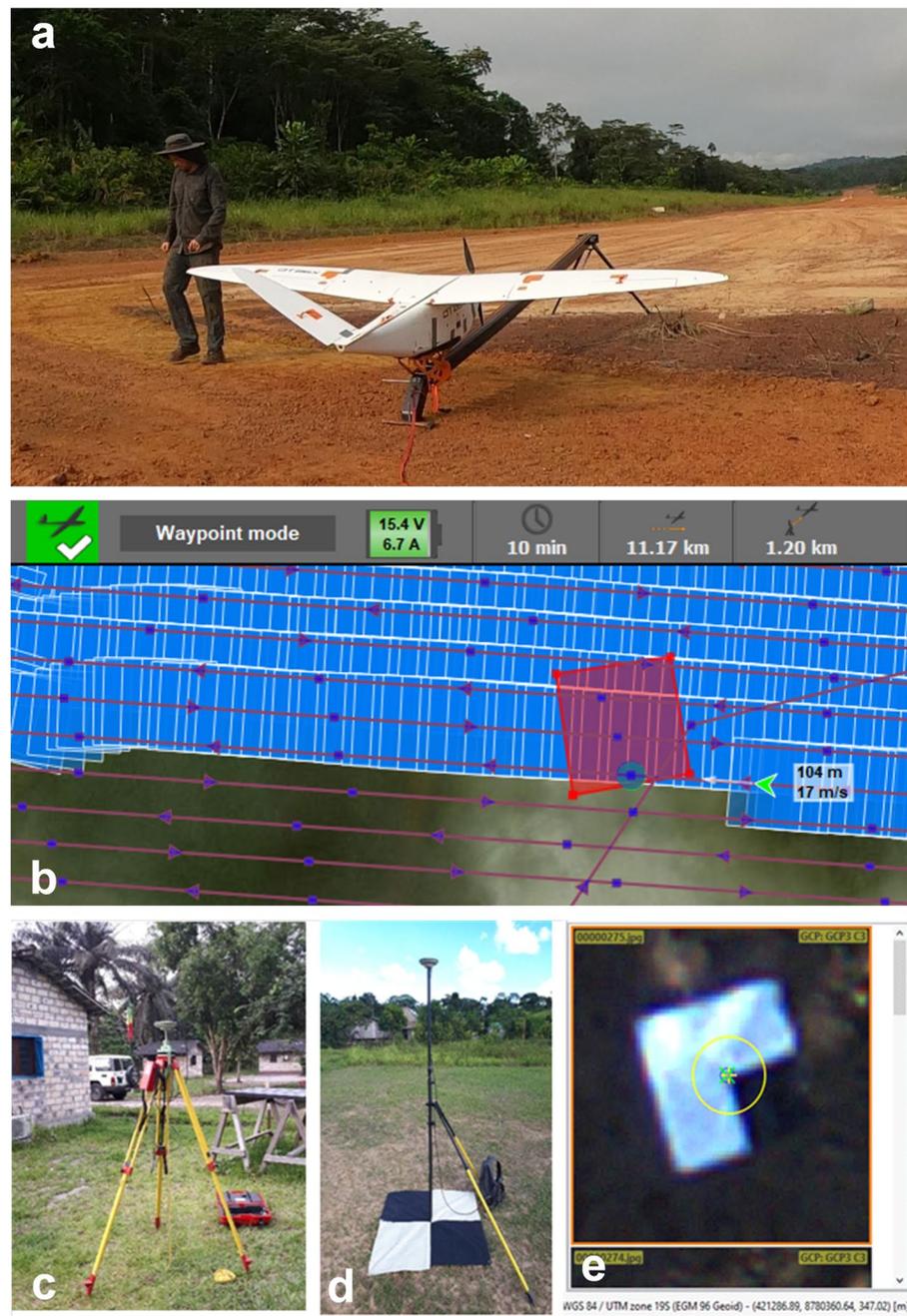
Figure 2. (a) The UAV prepared for launch in Gabon, using conventional take-off and landing (CTOL) procedure aided by a catapult. (b) An example mission over the same study area with flight lines and an approximate image footprint. (c) A static GNSS receiver, the data from which is used to correct the flight trajectories, with additional refinements and corrections possible via ground control points (d + e), located across the study area, the location of which are measured using a "rover" GNSS receiver.

A temporary GNSS base station (LEICA) was established at each site and initially left to collect data for 24 h to derive an accurate and precise position. The receiver is set to record in sync (1 measurement/s) with the UAV, and was set to run for an hour before and after each day's missions to allow PPK correction. A minimum of three Ground Control Points (GCPs)-square targets 1–2 m^2 composed of alternating black and white material arranged in a checkerboard pattern—were placed across the road/track network to allow further correction of the flight trajectory and support co-registration during the processing of each mission. Additional marker points, such as

buildings and other invariant objects (e.g., solar panels, road marker posts) were used to refine and check the accuracy of the final data sets. These were geo-located using a secondary "rover" GNSS receiver referenced back to the base station (Figure 2).

All flights were conducted in perpendicular lines and at a nominal altitude of 100–130 m above the ground surface with an average flight speed of 17 m/s (60 km/h). For the LiDAR, this results in a swath width of 100 m, with an average flight line spacing of 25 m (based on a target 70%–80% side overlap), and a maximum laser beam footprint at the ground level of 20–30 cm, reducing to 10–15 cm at 50 m. For the RGB data, the altitude and field of view mean each image covers an area $\sim 80 \times 70$ m in size, with a side and front overlap of 70% and 75% respectively meaning each area was imaged ~ 8–$10x$ with a ground sampling distance (GSD) of 3 cm per pixel. The flight parameters were chosen to maximize information content in both the LiDAR and SfM-DAP data sets; however, for the latter, it should be noted that the degree of image overlap and the resultant GSD, whilst sufficient (see next section), should be considered the minimum when working over dense vegetation (Assmann et al., 2019; Iglhaut et al., 2019).

The data used in this study comprises a total of 15 missions conducted over the course of 7 days in Peru and 3 days in Gabon. All data were principally collected in the morning between 8 and 11 a.m. in an attempt to obtain consistent light conditions between missions, and to avoid solar hotspots and the typically high temperatures (>30°C) after solar noon. However, given the size of the study area and the large distances traveled by the UAV from the operator (1–7 km), combined with the relatively long flight times (45–75 min), recording and controlling for light conditions was not possible meaning there are undoubtedly some differences within and between missions. It is important to note that special permissions were sought and obtained for flying Beyond Visual Line of Sight, which may or may not be possible in certain contexts, particularly if flying close to population centers.

2.3. Data Processing

The flight trajectories were reconstructed using the GNSS/IMU measurements and adjusted using the differentially corrected base station data within the Applanix POSPac Software. The corrected flight paths and laser data were combined using the RIEGL software package, RiPROCESS to generate the initial laser 3D point cloud. Residual errors in the flight trajectory, for example, due to discrepancies in GPS tracking and elevation, were corrected using small buildings to guide additional adjustments to the relative position and orientation of individual flight lines/scans. The trajectories were further refined using the GCPs resulting in a final LiDAR-derived point cloud with a geometric accuracy of 1.8 cm. The images were processed using the Pix4DMapper software (Pix4D, Lausanne, Switzerland; v. 4.4.12) and were sharpened prior to analysis. The process is largely automated and broadly follows the guidance set out by the software provider based on the vegetation type, flight plan, and sensor rig used. A more detailed description of the theoretical principles and techniques can be found elsewhere (Iglhaut et al., 2019; Westoby et al., 2012), however, in short, the processing chain first identifies points or sets of pixels with a distinctive and similar texture from sets of overlapping images. We used a custom matching procedure that leveraged the accurate geolocation of the images to ensure pairs were selected based on triangulation of proximal images, as well as capture time. An iterative bundle adjustment then refines the initial camera parameters, using the corrected positions and orientations of each image as a starting point, to derive an initial point cloud consisting of key points matched in different images. The GCPs were then manually identified and marked in all available images to aid the optimization before a multi-stereo algorithm generated a densified point cloud containing estimated 3D point positions. All elevation data were calculated according to the ellipsoidal height (m), with the Peru processed in WGS84 UTM 19S and Gabon in the UTM 33S coordinate system respectively. Each flight was processed separately with all data sets merged before being exported. All subsequent processing of the points clouds was done using elements of the lidR package (V3.1.0; Roussel et al., 2020).

Point clouds were filtered to remove outliers using a two-step approach; first, discontinuities in height profiles were used to identify and remove isolated clusters of points clearly separated, that is, >5 m difference in height, from the remainder of the point cloud, a feature that was more apparent in the image-based point clouds. The mean Euclidean distance between each remaining point and its 10 nearest neighbors was then calculated and if this value exceeded 2 m, the point was considered an outlier and removed. Filtering was conducted in 0.25 ha (50×50 m) segments to limit topography affecting the height profiles. Point clouds were thinned using 10 cm voxels to account for differences in sampling intensity between areas, which will more likely affect the LiDAR data. The final voxelized LiDAR point clouds have a mean density of 220 pts m^2 in Peru, and 240 pts m^2 in
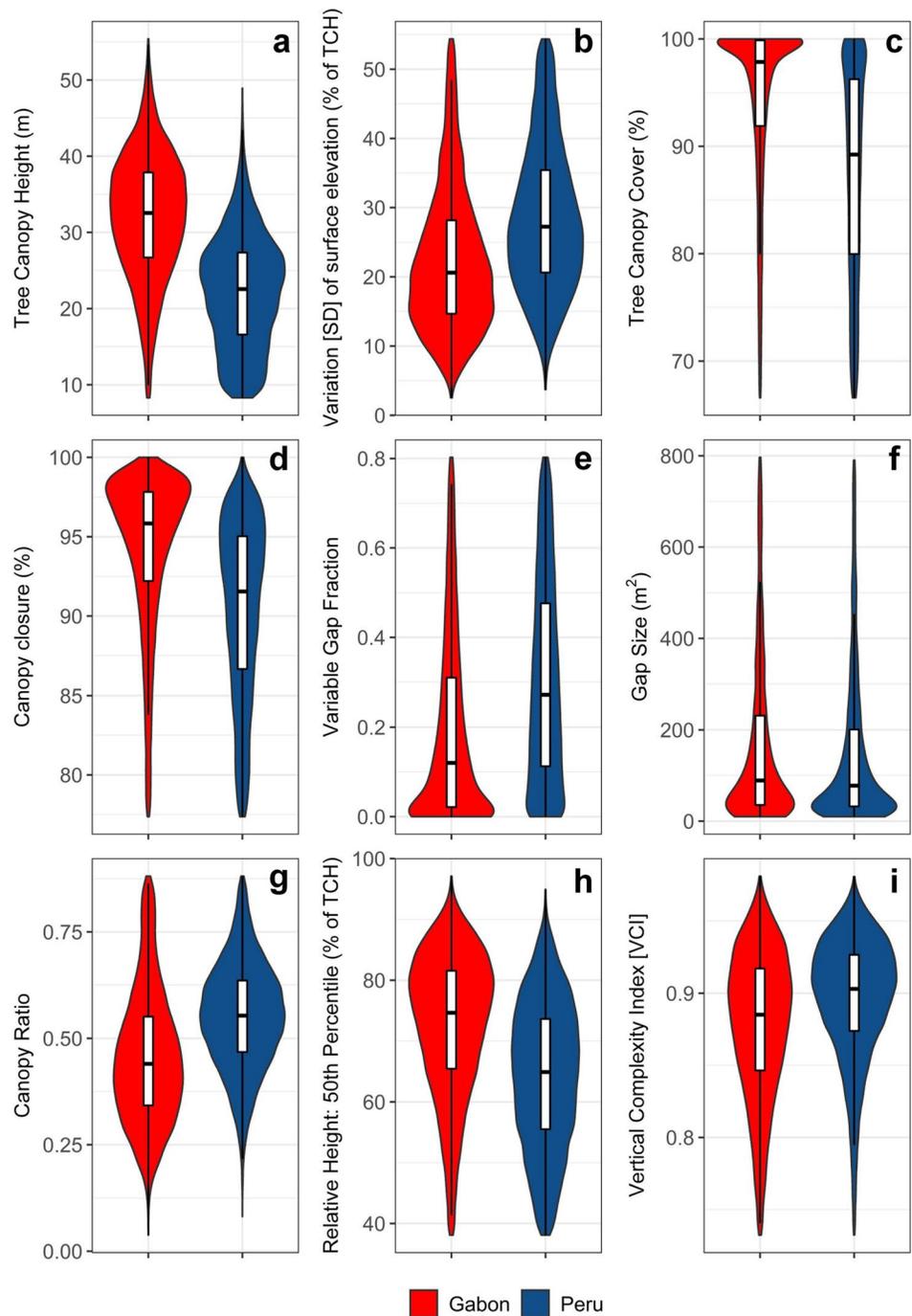
Figure 3. Comparison of key metrics describing forest structure across the study areas in Gabon and Peru as measured by the LiDAR sensor. Measurements of surface rugosity (b), and Relative Height (g) are expressed relative to the corresponding mean top of canopy height. Outliers are not included.

Gabon, while for the DAP data sets, it is 210 and 140 pts m² for Peru and Gabon respectively (Figures 2 and 3). We exclude areas with densities <10 pts m² within a 10 × 10 m² moving window, which includes areas toward edge of the data set, and gaps between flight lines where data quality was deemed to be low, leaving a total area coverage of 1,100 ha in Peru and 655 ha in Gabon.

2.4. Forest Structural Metrics

We selected a range of metrics considered important for area-based AGB estimation, and for measuring various aspects ecosystem structure and function. All data sets are gridded and presented in the main text at 20 m (0.04 ha) resolution, with the agreement of different data sets assessed according to the Concordance Correlation Coefficient (CCC), the Mean Error or Bias, and the Root Mean Square Error (RMSE), expressed in both absolute terms and relative to the LiDAR-derived values.

The first variable we compare is mean *Top-of-Canopy Height* (TCH), and its spatial heterogeneity or *Rugosity*, both of which are key variables in the area-based estimation of AGB (Asner & Mascaro, 2014; Bouvier et al., 2015; Jucker et al., 2017; Knapp et al., 2020). Ground returns were identified by extracting the lowest returns within a 1 m grid, and then applying a cloth simulation filter (Zhang et al., 2016) to separate ground from non-ground points. These were aggregated to create an average ground elevation for comparison. First returns were extracted (canopy surface elevation) and compared with the coincident ground elevations to generate an estimate of TCH, which along with canopy surface elevations, were averaged during the aggregation. The variation in surface height, sometimes referred to as rugosity, were calculated as the standard deviation of heights in each grid, although alternatives measures of spread have also been suggested and applied (e.g., Coefficient of Variation and Gini Coefficient; Bouvier et al., 2015; Knapp et al., 2020). For these direct comparisons, no interpolation, or averaging was used with areas of no data excluded from all subsequent comparisons between methods and sensors.

The second set of variables are related to tree canopy cover, and its inverse, canopy gap fraction, for which multiple definitions and measures exist. Canopy cover, or the number and size of canopy gaps are a keystone, and widely used descriptor of ecosystem structure. This information is important when assessing the ability of different data sets to correctly detect non-stand replacing disturbances, such as low intensity logging, or monitor smaller changes related to tree growth and mortality (Asner et al., 2013; Dalagnol et al., 2021; Goodbody et al., 2020; White et al., 2018). The first metric we compare is *Tree Fractional Cover*, defined as the proportion of the ground surface covered by the vertical projection of the tree canopy, based on a 1 m canopy height model (CHM) and a fixed height threshold of 10 m. This has been used as a predictor of basal area for use in AGB estimation (Coomes et al., 2017; Fischer et al., 2019; Jucker, Asner, Dalponte, Brodrick, Philipson, et al., 2018), and as a proxy for disturbance impacts on tree structure (Almeida et al., 2019). An alternative measure is *Canopy Closure* (*sensu* Jennings et al., 1999), defined as the proportion of the sky hemisphere obscured by vegetation from a single point on the ground and measured here as the proportion of the total points in each grid cell above the same 10 m canopy height threshold. Given data were collected from multiple viewpoints, this metric is better suited to fractional cover when comparing LiDAR and DAP, and the extent to which the sub-canopy or ground surface is likely to be visible.

In this context, we also created data sets describing gap fraction, which includes information on gap size given that smaller, isolated canopy gaps are unlikely to allow sufficient illumination of the sub-canopy. We used the methods contained in the ForestGapR package (Silva et al., 2019), with the same fixed canopy height threshold of 10 m used to separate tree canopies from gaps (*Fixed Gap Fraction*) (Dalagnol et al., 2021), but with an additional minimum size threshold of 10 m^2, and a maximum of 2 ha to exclude small isolated gaps and naturally open areas respectively. Small linear gaps (~10 m^2), for example, between tree crowns, were removed as they often connected large canopy gap openings meaning their calculated size is misleading, and led to true gaps exceeding maximum size threshold. We also applied a variable height threshold (*sensu* Dalagnol et al., 2021; White et al., 2018) classifying an area as a gap if its canopy height is less than 50% of the corresponding maximum height within a 50×50 m (0.25 ha) window (*Variable Gap Fraction*). This measure is better for capturing small discontinuities or temporal changes in tree canopy cover (Dalagnol et al., 2021), particularly where disturbance impacts are minimal, or have been obscured via regrowth in the sub-canopy. In both cases, a smoothed digital surface model (DSM) was generated at 1 m resolution to avoid no-data areas in the image-based point clouds being incorrectly labeled as a gap, based on the "pitfree" method from Khosravipour et al. (2014). For this, ground returns were interpolated using the 20 nearest neighboring points, located within a 50 m radius to create a 1 m Digital Terrain Model (DTM) which was subtracted from the DSM to create a smoothed top-of-CHM.

The final set of variables describe vertical forest structure and the ability of different methods to capture the variation and number of canopy layers. Each metric is applied to the vertical point cloud profiles separated in to
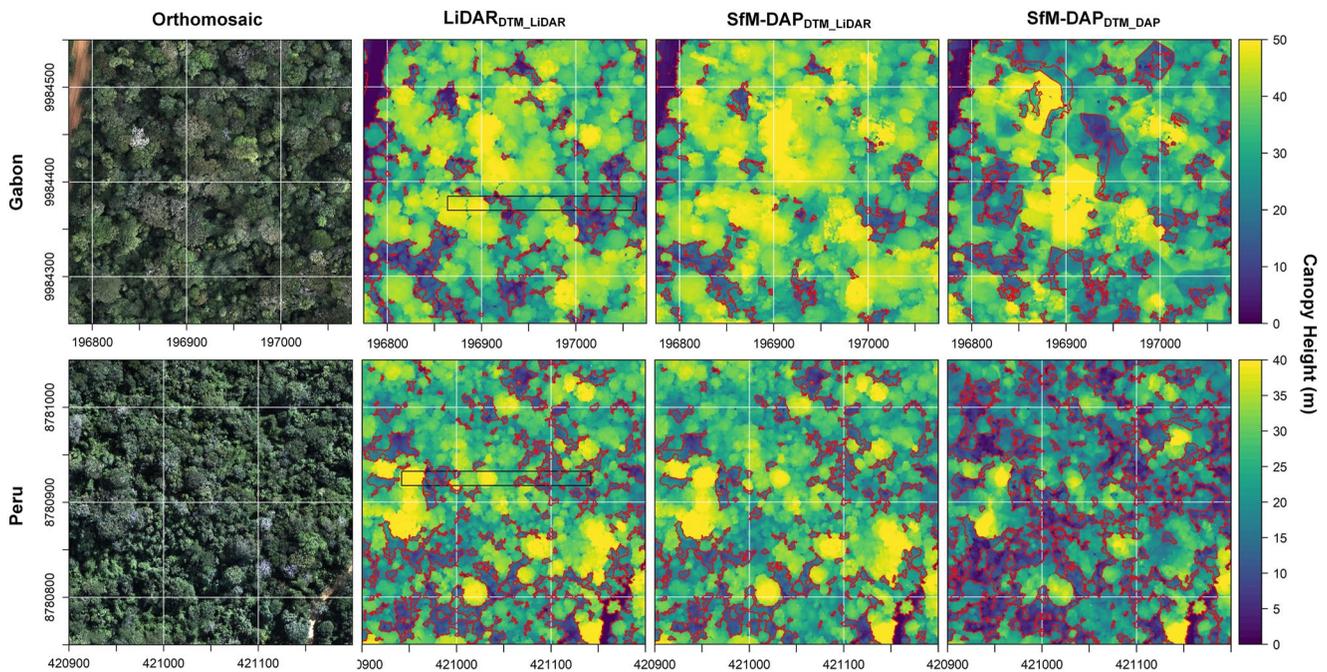
Figure 4. A comparison of canopy height models (CHM) across a 9 ha patch of forest obtained via LiDAR, and the DAP-based points clouds, with tree heights estimated using both the LiDAR-derived DTM, and using the estimated ground elevations from the DAP data directly. Red polygons indicate gaps detected via the Variable Gap method, that is, areas where canopy height is <50% of the maximum height within a 50 × 50 m moving window. Transects delineated in the LiDAR CHM show the location of 3D vertical profiles in Figure 5.

1 m height bins (Figure 3). The first of these is the *Vertical Complexity Index (VCI)* or *Entropy,* which measures the diversity and the evenness of points within a vertical profile based on the Shannon Diversity Index ("entropy" function; lidR), with higher values (0–1) reflecting a more uniform distribution of points. The next set of metrics are the *Relative Height (RH)* percentiles, which refer to the heights within a vertical profile at which a given percentage of points are located below that value. We extracted the 5th–95th percentiles, and from these calculated the *Canopy Ratio* (Schneider et al., 2020), which is measured as: (RH95–RH25)/RH95 and describes both the ratio between vegetation depth and height, and the skew in point densities. High values typically result from a more complex forest structure (i.e., caused by multiple canopy layers), and are considered a good indicator of habitat quality for plants and animals (Burns et al., 2020; Schneider et al., 2017, 2020). These and other metrics that use RH data also form a key part of models for estimating AGB (Dubayah et al., 2020; Meyer et al., 2013).

3. Results

3.1. LiDAR-Based Measurement of Forest Structure

Forest structure varied markedly across, and between the two study regions, with TCH in Gabon reaching 35–50 m in areas with a fractional cover >50%, compared to 25–40 m in Peru (Figures 3 and 4). Despite their relatively low stature, the Peruvian forests are more structurally complex, with vertical profiles capturing the known sub-canopy layer 10–15 m in height (Figures 1 and 3), and metrics describing vertical structure also indicating a greater density and more even spread of vegetation (Figures 3f–3h). These patterns contrast sharply in Gabon where there is typically a single dominant tree layer varying little in height (Figures 3a–3c). The relatively low variation in tree height means fewer areas are identified as gaps, as detected using the variable height method, with 7% of the forest area in Gabon identified as such (log-transformed mean size: 91 m^2), compared to 20% in Peru (113 m^2) (Figures 4 and 6). Canopy gaps measured using a fixed height threshold (10 m) were rare, comprising <5% of the forest area at either site, and by definition were correlated with tree fractional cover meaning these are not considered further.
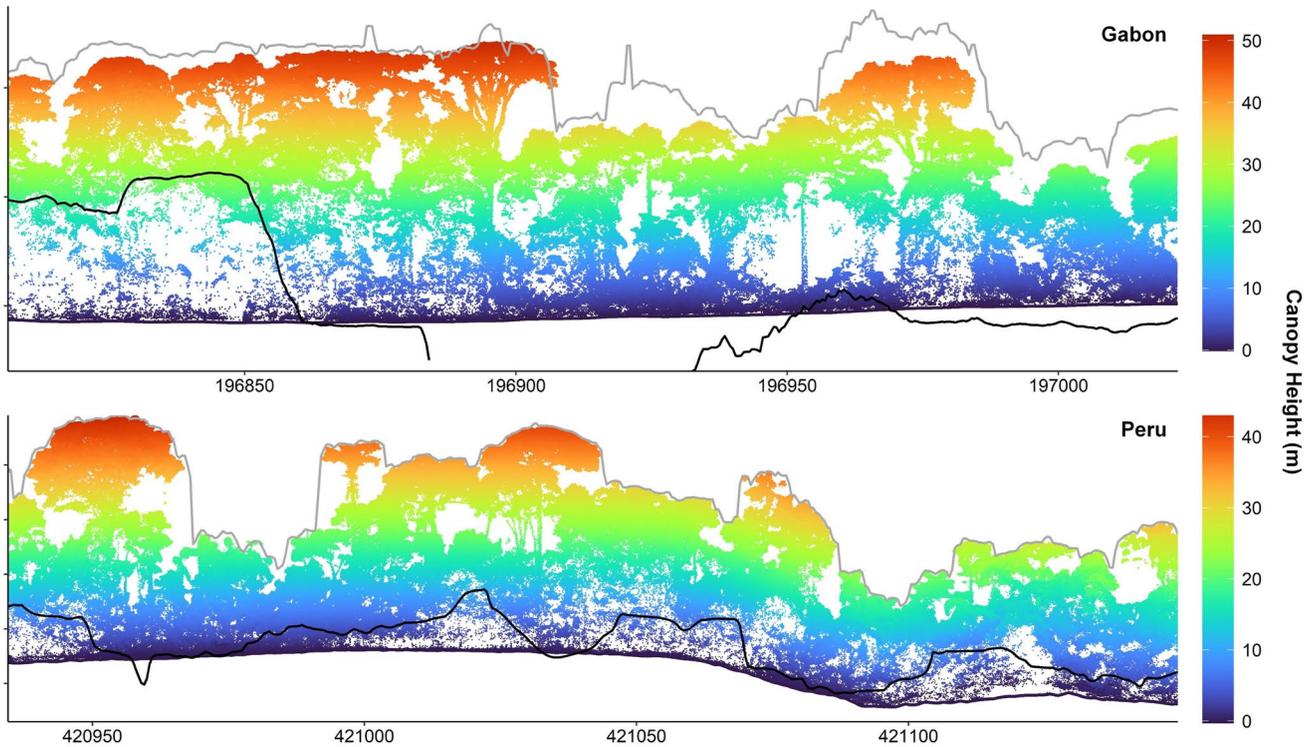
Figure 5. Example 3D LiDAR point cloud profiles, with black lines showing the SfM-DAP DTM, and the gray lines the DAP DSM for the same area.

3.2. Comparison of LiDAR and DAP Metrics

Many of the broad patterns in forest structure observed on the ground, and in the LiDAR data, are also apparent in the SfM-DAP derived point clouds (Figures 4 and 6). Measurements of surface elevation and its variability/rugosity showed good correspondence (CCC: 0.99), varying by maximum 1–2 m between methods (Figures 4 and 7). However, the ability of SfM-DAP to extract information from lower in the canopy, including ground returns (CCC: 0.42), becomes increasingly limited in areas with higher canopy cover (>70%), which comprise the majority of both study areas. Consequently, we find large, but variable differences in TCH (Figure 7), with individual estimates lower by an average of 6 m (RMSE: 11.6 m) in Gabon, and 8 m (RMSE: 10.0 m) in Peru, equivalent to an 18% (SD: 36%) and 40% (26%) underestimation of TCH relative to the LiDAR estimates (Figure 8). For Peru, the relative bias on TCH was consistent up to 80%–90% cover, after which estimates decrease rapidly, falling to <50% of the LiDAR measurements (Figure 8). An almost identical pattern was observed in Gabon, with errors increasing exponentially as canopy closure exceeds 90%, however, over-estimation of TCH was also common (Figure 5), resulting in more comparable, but highly variable estimates in the small number of areas with moderate tree cover (<80%). Areas with higher surface rugosity were associated with progressively more comparable estimates of TCH, likely through reductions in occlusion and greater illumination of the sub-canopy, however, we found no trend with increasing gap fraction, or gap size (Figure 8).

These differences in ground elevation, and therefore TCH, have clear implications for other metrics that use this information in their derivation (Figures 7e–7l); indeed, there is a tendency for DAP to overestimate both the variable gap fraction (%Bias: Gabon = 40%; Peru = 37%) and the size of these gaps (200%; 91%), and to underestimate tree fractional cover (−15%; −40%) and canopy closure (−7%; −29%). As with TCH, larger discrepancies were typically in areas with lower surface rugosity, and high canopy closure, due to the associated negative bias on tree heights (Figure 8). We find a similar skewed distribution for metrics describing vertical structure, including vertical complexity/entropy, and RH values (Figure 7), however, for each, the overall bias was relatively small with estimates typically within 10%–20% of the LiDAR-derived values (Figures 5–7). In general, the RH values for mid- to upper canopy (RH50–RH95) are similar between methods, although the greater density of ground returns in the LiDAR results in greater divergence lower in the canopy profile (Figure 6). Crucially, we find that incorporating the LiDAR ground elevations in to the DAP point clouds reduced the overall bias in tree fractional
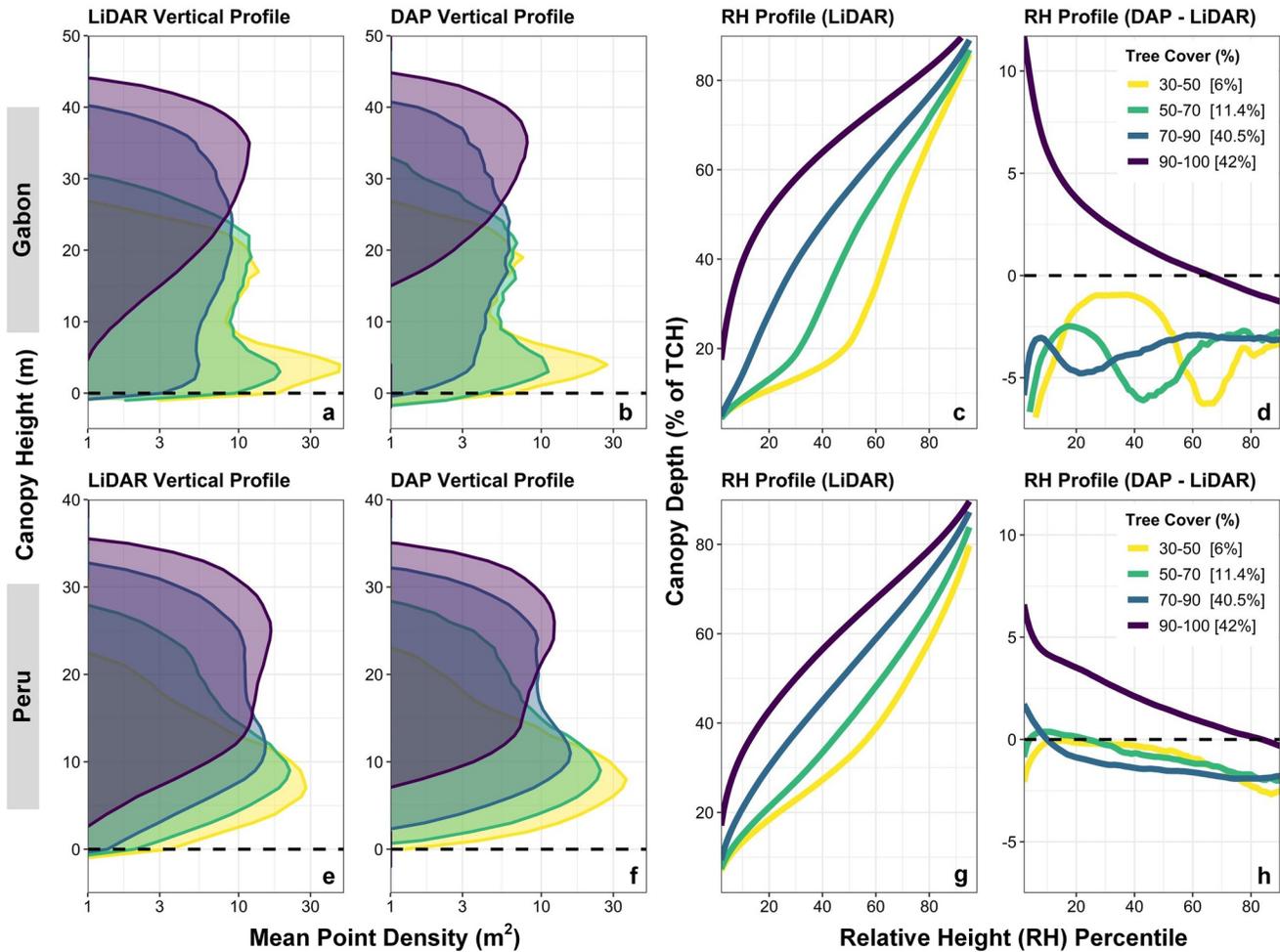
Figure 6. The four panels to the left (a), (b), (e), (f), show the vertical point density profiles (1 m height bins) from the LiDAR, and DAP derived point clouds, averaged across each study area, and separated by Canopy Closure (%). The data were extracted within 20 × 20 m grids, with the values in square brackets the percentage of each study area with the corresponding canopy closure. The remaining four panels on the right (c), (d), (g), (h) show the averaged RH profiles for the LiDAR data (c), (g), with heights expressed as a proportion of the TCH in each grid cell, and the difference to the DAP data (d), (h).

cover, canopy closure, and gap fraction (Figure 8). However, there are differences that canopy height cannot account for, with DAP predicting gaps where none, or few exist in the LiDAR data. Importantly, we find the RH values, and the VCI, were broadly unaffected by the inclusion of a more accurate DTM (Figure 8), indicating such information can be extracted independent of LiDAR with a similar degree of precision and accuracy.

4. Discussion

In this study, we examined to what extent information on 3D forest structure obtained via DAP and structure-from-motion techniques (SfM-DAP) can replicate that obtained from a LiDAR sensor. These data sets were obtained simultaneously using an UAV, which due to their ability to fly low and image the same area from multiple oblique viewpoints, have the potential to provide a much improved and novel basis for evaluating the capacity of image-based methods. We compared various metrics of canopy and vertical forest structure demonstrated as important for AGB estimation, and/or for measuring various aspects of ecosystem structure and function, including proxies for habitat quality and biodiversity. These data were collected over two contrasting areas of tropical forest; one in central Gabon, where forests are typically characterized by a single layer of relatively tall trees (TCH: 30–50 m), and the second in Peru, where the forests are structurally more complex, with multiple canopy layers (TCH: 25–40 m).
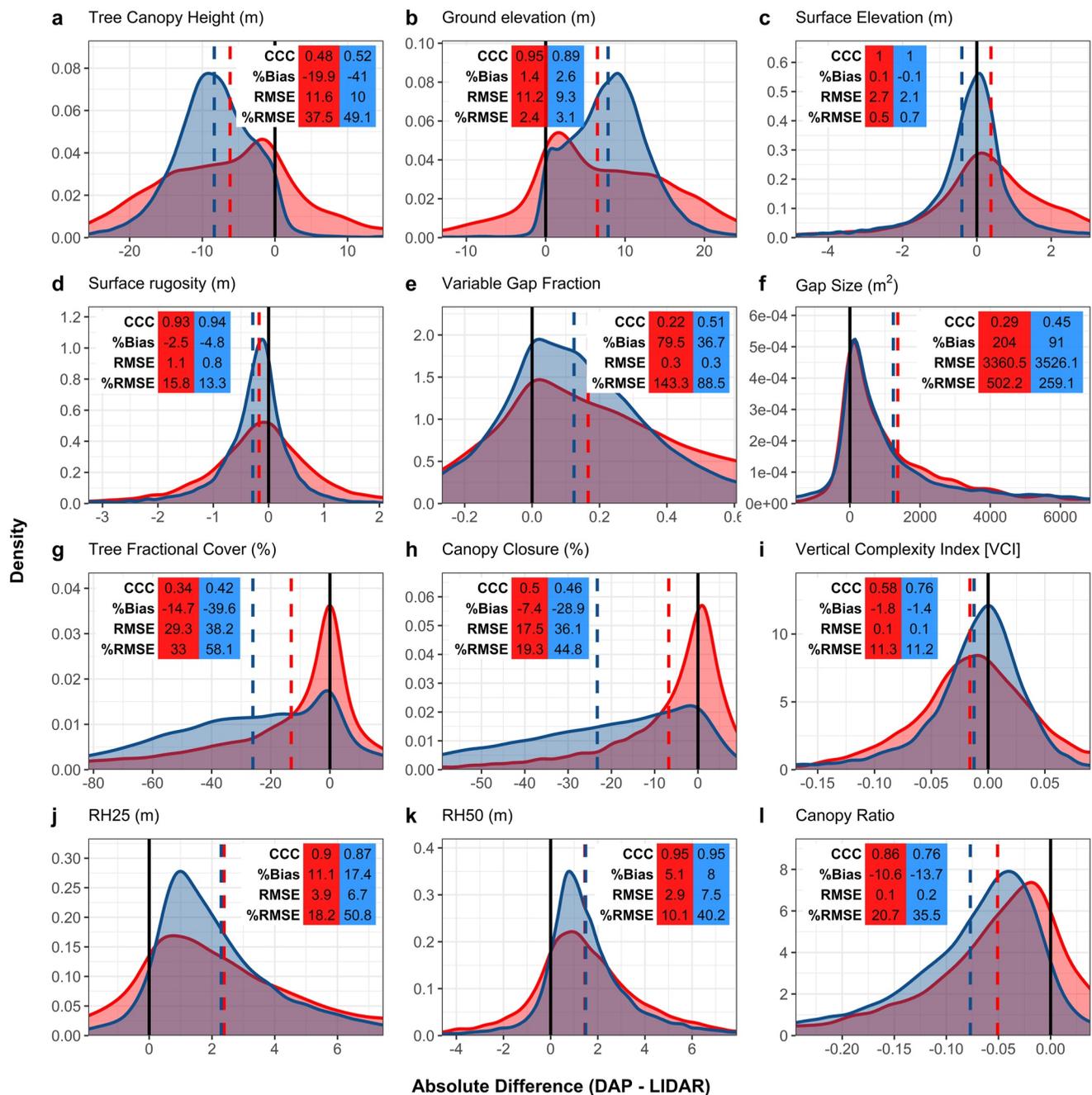
Figure 7. The absolute difference between the LiDAR and SfM-DAP derived estimates of forest structure from across the study areas in Gabon (red) and in Peru (blue). The x-axis limits encompass up to 95% of the data at either study site. Summary statistics include the mean error, or bias, for each data set, and is shown by the vertical hatched lines. The inset tables present the mean bias in relative terms (to the mean of the LiDAR data), and the RMSE in absolute and relative terms.

We show that SfM-DAP derived point clouds cannot be used in isolation to generate accurate estimates of TCH—a central variable in LiDAR-AGB allometric models (Asner & Mascaro, 2014; Jucker, Asner, Dalponte, Brodrick, Christopher, et al., 2018; Knapp et al., 2020)—due to the difficulties in extracting accurate estimates of ground elevation. Our results broadly echo the conclusions of previous studies, including those working in tropical forests (Swinfield et al., 2019; Vaglio Laurin et al., 2019), leading to suggestions that image-based methods are (a) only permissible in more open forest stands, for example, those with <50%–60% canopy cover (Mlambo et al., 2017; Wallace et al., 2016), or (b) only suitable for conducting measurements in areas with existing digital elevation models (DTMs), such as those obtained via LiDAR (Goodbody et al., 2019; Vaglio Laurin et al., 2019;
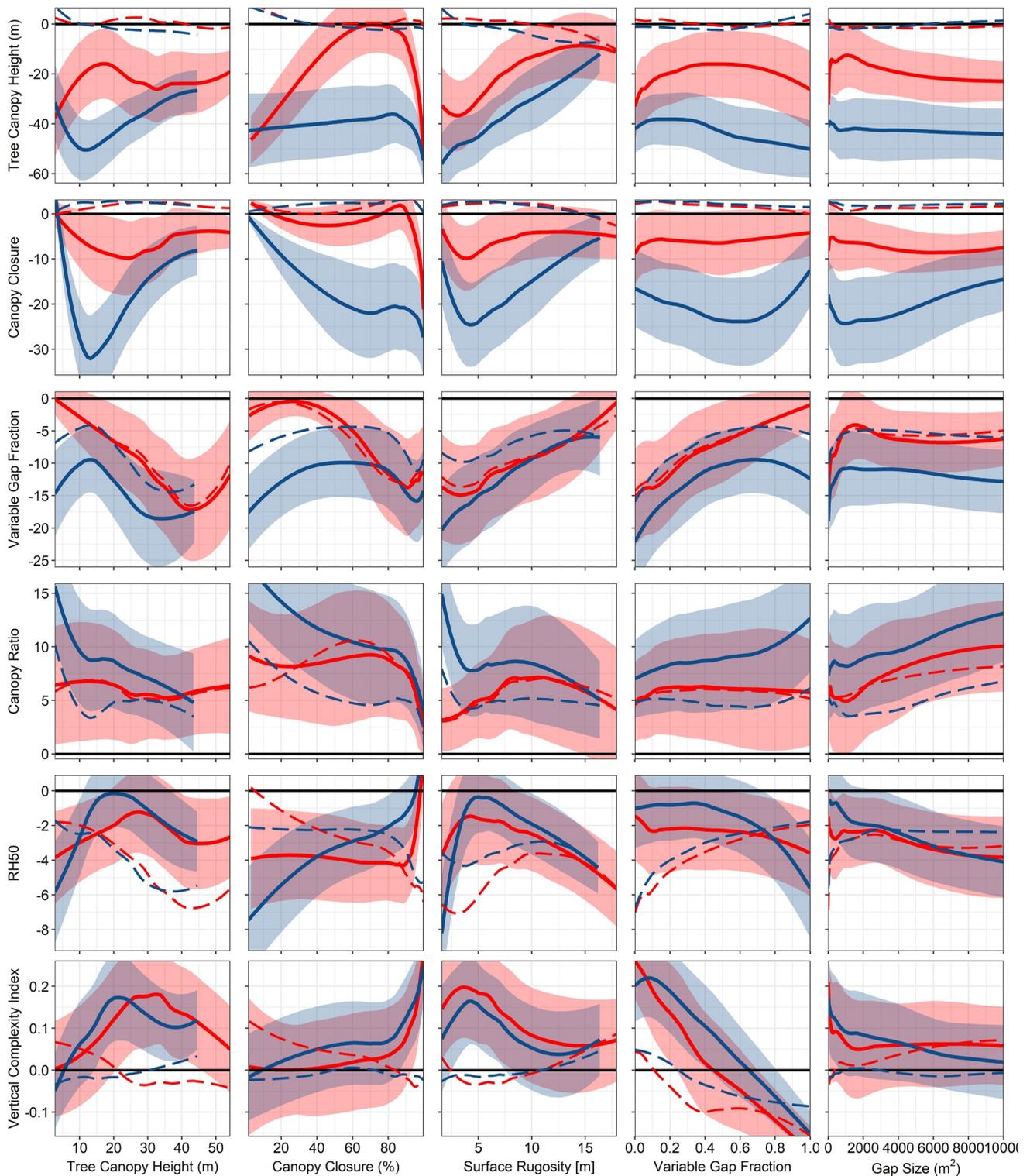
Figure 8. The differences between the SfM-DAP and LiDAR measurements (*y*-axis) of horizontal and vertical structure as a function of various descriptors of tree canopy structure, created using the LiDAR point clouds (*x*-axis). Here, differences are expressed according to the relative error, or %Bias, with the exception of Variable Gap Fraction and Canopy Closure which is the absolute difference (Figure 7). The solid lines refer to the SfM-DAP data used in isolation, while the hatched lines show the trend using the LiDAR DTM corrected SfM-DAP data. The relative bias was smoothed using a LOESS (locally weighted scatterplot smoothing) procedure. The error bars encompass half of the SD to better display both the average trend, and the range of estimates for a given context, with the upper and lower bounds also smoothed using LOESS.

White et al., 2013). In this article, we examined both of these assertions due to the scale of our data sets (100s ha), and the varying vegetation types and densities present within the two study areas.

Overall, the size of the underestimation on TCH was highest at the site in Peru, where estimates were 40% lower than the LiDAR values, compared to 20% in Gabon. The size of the underestimation in TCH increased markedly in areas where canopy closure exceeded 80%, which account for large proportion of the forest area at both study sites. However, even in more open areas, there still exists large, and, inconsistent differences (40%–50% RMSE) between the SfM-DAP and LiDAR-derived estimates of tree height, even in areas with low to, non-existent tree cover, or in areas with larger canopy gaps. That these differences are inconsistent is important as it prevents bias-correction of the TCH based on a local LiDAR (or other tree height) data set. In Peru, the presence of a clear sub-canopy, and relatively dense ground vegetation layer seemingly precludes accurate ground detection using SfM-DAP. In Gabon, the estimates were more comparable, particularly in the relatively small number of more open forest patches, albeit with greater tendency for SfM-DAP to overestimate tree height. Observations of the imagery suggest the combination of tall trees, lower surface rugosity, and by extension, the lower gap fraction creates insufficient illumination, and thus darker patches resulting in lower estimates of ground elevation (White et al., 2018). Our results, and interpretation diverge from those detailed by Swinfield et al. (2019), who showed that DAP systematically underestimated TCH among recovering secondary forests in Indonesia, and presented a simple linear model to correct these estimates. Adopting a similar approach is complicated by the comparatively weak, and variable correspondence between measures of TCH, which when coupled with the nonlinear effect of canopy closure, and influence of surface rugosity, suggests that a more complex model would be required to properly account for these uncertainties across these landscapes. Other potential sources of random error/variation in the data include the intensity and angle of solar illumination when the data was acquired (Gobakken et al., 2015; Roşca et al., 2018), which is hard to control for in tropical forests, or when collecting measurements over large areas due to frequent and rapidly changing cloud cover. This complexity is acknowledged in Swinfield et al. (2019), who notes that local refinement and calibration of the model would be required along with the collection of independent height data, likely from LiDAR, which would largely negate the need for a corrective model assuming ground data can be reliably obtained across the area of interest.

However, despite the clear, and widespread difficulties in measuring ground elevation, SfM-DAP can be an effective method for retrieving information on top-of canopy structure including surface elevation and heterogeneity (Gobakken et al., 2015; Roşca et al., 2018; St-Onge et al., 2008; Swinfield et al., 2019). This is important as it suggests that in areas where an accurate DTM is available, for example, from a previous (but non-repeatable) airborne or UAV LiDAR campaign, SfM-DAP can be used to reliably extract information on canopy height, heterogeneity, and fractional cover, all of which are key predictor variables in commonly applied area-based LiDAR-AGB allometric models (Asner & Mascaro, 2014; Jucker, Asner, Dalponte, Brodrick, Christopher, et al., 2018; Knapp et al., 2020). However, the need for an accurate DTM negates many of the unique benefits of using SfM-DAP over LiDAR. For that reason, Giannetti et al. (2018) developed new models for predicting stem volume in Italy and Norway using DTM-independent variables alone, producing estimates with similar accuracy to LiDAR data, even in areas with steep terrain. The creation and testing of models that do not require a DTM would be an important addition to the literature and should allow data collection in areas where more expensive LiDAR (or no data collection at all) might have been the alternative.

Despite the close correspondence in surface heights, the results of this study also demonstrate some potentially important, albeit minor differences between the surface models (DSM) obtained from LiDAR and SfM-DAP data, particularly in the detection of canopy gaps. Prior to this study, the relative capacity of SfM-DAP data to capture canopy gaps in complex tropical forests had not been investigated and compared to LiDAR data. Again, the results show that incorporating an accurate DTM greatly reduces the bias on measures of canopy gap fraction, resulting in broadly consistent estimates between methods, thus highlighting the capacity of SfM-DAP to capture these data. However, the results also suggest a tendency for SfM-DAP to detect openings in areas where the LiDAR data does not, or where the detected gaps are small (<100 m^2). Although these differences are minor, they are potentially important when considering the ability to capture and monitor changes associated with small-scale logging, or mortality (Dalagnol et al., 2021). The results may be improved upon by increasing the front- and side-overlap in the imagery to 80%–85% (e.g., by increasing altitude, and/or flying slower), which may result in better reconstructions by increasing the GSD and potential number of matches, particularly in areas where the vegetation is more uniform, like in Gabon where the SfM-DAP surface models were more variable relative to

LiDAR. That being said, our data could also be considered optimal, given the accurate geolocation of the images through PPK correction which may not be possible with lower cost platforms and sensors. The use of GCPs should improve reconstructions, however, this also requires survey grade GNSS receivers to differentially adjust the data, and their placement in dense forest areas can be challenging. It is, therefore, possible that the quality of the DSMs produced by SfM-DAP will be lower in some cases.

The final set of comparisons were for metrics describing vertical structure. We posited that UAVs may provide new insights into the capacity of DAP to capture the vertical profile due to their ability to fly low (relative to aircraft), and view the forest from multiple oblique angles. Indeed, we find that each measure of vertical structure, most notably the RH percentiles, and associated metrics, were similar, and in some near-identical between methods, with values from the DAP point clouds within 5% of the LiDAR-derived values. This novel finding most likely reflects that even with UAV-borne LiDAR, a small proportion of total returns are located close to, or at the ground surface (1–10 pts m^2), which although critical for estimating ground elevation, results in a small difference in RH percentiles compared to SfM-DAP, which principally captures the outer envelope of the forest. For many, if not all ecological applications, errors of this size (<10%) may be considered acceptable, suggesting that DAP may be used as a direct substitute for LiDAR data, for example, as part of calibration models estimating AGB (Meyer et al., 2013; Qi et al., 2019), or perhaps more applicable, for mapping and understanding patterns in plant and animal diversity (Burns et al., 2020; Schneider et al., 2020). Again, there are some caveats to this interpretation, namely, that RH metrics and others based on vertical point profiles, are sensitive to the LiDAR sensor (e.g., power, beam divergence), and platform (e.g., flight speed, height) used to collect the data. Similarly, in the case of SfM-DAP, methods used to generate image-based point clouds may differ significantly between software, and versions, although any sensitivity is hard to predict as the underlying algorithms are proprietary and a black box to the scientific community. These differences may be minor, however, it is proposed that metrics derived from SfM-DAP data should only be transferred to existing models in areas where correspondence to the data underpinning the original model is already established, as demonstrated by Tompalski et al. (2019).

Overall, our results help to reinforce the ever growing body of literature pointing to SfM-DAP as a viable alternative to LiDAR for the extraction of key metrics of forest structure, particularly in areas with existing data on ground elevation. The decision on whether to apply SfM-DAP based methods must consider not only the costs of data acquisition and processing, but also the potential uncertainties in the approach, and the full value of the information provided. Although it is clear from our results that some area-based metrics are likely to be comparable between methods, it is important to note that LiDAR is capable of generating more detailed information on forest structure, including models of crown structure and depth, and the segmentation of individual trees, even in relatively dense forests (Brede et al., 2017). This is significant when considering the relative importance of area-based vs. individual-based methods of mapping AGB in dense tropical forests. Current data suggests that area-based methods tend to out-perform more complex attempts to segment and model individual trees in tropical forests, largely due to difficulties in separating overlapping tree crowns, and detecting lower vegetation (Coomes et al., 2017). However, the increasing use of UAVs equipped with powerful LiDAR sensors, including the one used here, means we now have the potential produce similar levels of detail to Terrestrial Laser Scanners, certainly for the upper canopy, which coupled with improvements to tree segmentation algorithms (Ferraz et al., 2020; Williams et al., 2020), have the potential to allow a more direct, or accurate estimation of canopy and/or tree volume, and thus AGB. As such, we assert that LiDAR should remain the preferred source of information on forest structure, however, in areas with existing terrain models, we show that SfM-DAP can be used to generate much-needed information on forest structure needed to better understand vulnerable and understudied forested ecosystems around the globe.

Data Availability Statement

The underlying data is available from the University of Edinburgh DataShare service (https://datashare.ed.ac.uk/handle/10283/4116).

References

Ali-Sisto, D., & Packalen, P. (2017). Forest change detection by using point clouds from dense image matching together with a LiDAR-derived terrain model. *IEEE Journal of Selected Topics in Applied Earth Observations and Remote Sensing*, *10*, 1197–1206. https://doi.org/10.1109/jstars.2016.2615099

Almeida, D. R. A., Stark, S. C., Schietti, J., Camargo, J. L. C., Amazonas, N. T., Gorgens, E. B., et al. (2019). Persistent effects of fragmentation on tropical rainforest canopy structure after 20 yr of isolation. *Ecological Applications*, *29*, 1221–1235. https://doi.org/10.1002/eap.1952

Asner, G. P., Kellner, J. R., Kennedy-Bowdoin, T., Knapp, D. E., Anderson, C., & Martin, R. E. (2013). Forest canopy gap distributions in the southern Peruvian Amazon. *PLoS One*, *8*. https://doi.org/10.1371/journal.pone.0060875

Asner, G. P., & Mascaro, J. (2014). Mapping tropical forest carbon: Calibrating plot estimates to a simple LiDAR metric. *Remote Sensing of Environment*, *140*, 614–624. https://doi.org/10.1016/j.rse.2013.09.023

Assmann, J. J., Kerby, J. T., Cunliffe, A. M., & Myers-Smith, I. H. (2019). Vegetation monitoring using multispectral sensors—best practices and lessons learned from high latitudes. *Journal of Unmanned Vehicle Systems*, *7*, 54–75. https://doi.org/10.1139/juvs-2018-0018

Assmann, J. J., Myers-Smith, I. H., Kerby, J. T., Cunliffe, A. M., & Daskalova, G. N. (2020). Drone data reveal heterogeneity in tundra greenness and phenology not captured by satellites. *Environmental Research Letters*, *15*, 125002. https://doi.org/10.1088/1748-9326/abbf7d

Bayley, D. T. I., & Mogg, A. O. M. (2020). A protocol for the large-scale analysis of reefs using structure from motion photogrammetry. *Methods in Ecology and Evolution*, 1–11. https://doi.org/10.1111/2041-210x.13476

Beland, M., Parker, G., Sparrow, B., Harding, D., Chasmer, L., Phinn, S., et al. (2019). *On promoting the use of LiDAR systems in forest ecosystem research* (p. 450). Forest Ecology and Management.

Bouvier, M., Durrieu, S., Fournier, R. A., & Renaud, J. P. (2015). Generalizing predictive models of forest inventory attributes using an area-based approach with airborne LiDAR data. *Remote Sensing of Environment*, *156*, 322–334. https://doi.org/10.1016/j.rse.2014.10.004

Brede, B., Calders, K., Lau, A., Raumonen, P., Bartholomeus, H. M., Herold, M., & Kooistra, L. (2019). Non-destructive tree volume estimation through quantitative structure modeling: Comparing UAV laser scanning with terrestrial LiDAR. *Remote Sensing of Environment*, *233*, 111355. https://doi.org/10.1016/j.rse.2019.111355

Brede, B., Lau, A., Bartholomeus, H. M., & Kooistra, L. (2017). Comparing RIEGL RiCOPTER UAV LiDAR-derived canopy height and DBH with terrestrial LiDAR. *Sensors*, *17*, 1–16. https://doi.org/10.3390/s17102371

Burns, P., Clark, M., Salas, L., Hancock, S., Leland, D., Jantz, P., et al. (2020). Incorporating canopy structure from simulated GEDI LiDAR into bird species distribution models. *Environmental Research Letters*, *15*. https://doi.org/10.1088/1748-9326/ab80ee

Burt, A., Boni Vicari, M., Da Costa, A. C. L., Coughlin, I., Meir, P., Rowland, L., & Disney, M. (2021). New insights into large tropical tree mass and structure from direct harvest and terrestrial LiDAR. *Royal Society Open Science*, *8*.

Coomes, D. A., Dalponte, M., Jucker, T., Asner, G. P., Banin, L. F., Burslem, D. F. R. P., et al. (2017). Area-based vs. tree-centric approaches to mapping forest carbon in Southeast Asian forests from airborne laser scanning data. *Remote Sensing of Environment*, *194*, 77–88. https://doi.org/10.1016/j.rse.2017.03.017

Cunliffe, A., Anderson, K., Boschetti, F., Brazier, R., Graham, H., Myers-Smith, I., et al. (2021). Global application of an unoccupied aerial vehicle photogrammetry protocol for predicting aboveground biomass in non-forest ecosystems. *Remote Sensing in Ecology and Conservation*, 1–15.

Dalagnol, R., Wagner, F. H., Galvão, L. S., Streher, A. S., Phillips, O. L., Gloor, E., et al. (2021). Large-scale variations in the dynamics of Amazon forest canopy gaps from airborne LiDAR data and opportunities for tree mortality estimates. *Scientific Reports*, *11*, 1–15. https://doi.org/10.1038/s41598-020-80809-w

Disney, M. I., Boni Vicari, M., Burt, A., Calders, K., Lewis, S. L., Raumonen, P., & Wilkes, P. (2018). Weighing trees with lasers: Advances, challenges, and opportunities. *Interface Focus*, *8*. https://doi.org/10.1098/rsfs.2017.0048

Dubayah, R., Blair, J. B., Goetz, S., Fatoyinbo, L., Hansen, M., Healey, S., et al. (2020). The global ecosystem dynamics investigation: High-resolution laser ranging of the Earth's forests and topography. *Science of Remote Sensing*, *1*, 100002. https://doi.org/10.1016/j.srs.2020.100002

Espírito-Santo, F. D. B., Gloor, M., Keller, M., Malhi, Y., Saatchi, S., Nelson, B., et al. (2014). Size and frequency of natural forest disturbances and the Amazon forest carbon balance. *Nature Communications*, *5*, 1–6.

Ferraz, A., Saatchi, S. S., Longo, M., & Clark, D. B. (2020). Tropical tree size-frequency distributions from airborne LiDAR. *Ecological Applications*, 1–18.

Fischer, R., Knapp, N., Bohn, F., Shugart, H. H., & Huth, A. (2019). The relevance of forest structure for biomass and productivity in temperate forests: New perspectives for remote sensing. *Surveys in Geophysics*, *40*, 709–734. https://doi.org/10.1007/s10712-019-09519-x

Giannetti, F., Chirici, G., Gobakken, T., Næsset, E., Travaglini, D., & Puliti, S. (2018). A new approach with DTM-independent metrics for forest growing stock prediction using UAV photogrammetric data. *Remote Sensing of Environment*, *213*, 195–205. https://doi.org/10.1016/j.rse.2018.05.016

Gobakken, T., Bollandsås, O. M., & Næsset, E. (2015). Comparing biophysical forest characteristics estimated from photogrammetric matching of aerial images and airborne laser scanning data. *Scandinavian Journal of Forest Research*, *30*, 73–86. https://doi.org/10.1080/02827581.2014.961954

Goodbody, T. R. H., Coops, N. C., & White, J. C. (2019). Digital aerial photogrammetry for updating area-based forest inventories: A review of opportunities, challenges, and future directions. *Current Forestry Reports*, *5*, 55–75. https://doi.org/10.1007/s40725-019-00087-2

Goodbody, T. R. H., Tompalski, P., Coops, N. C., White, J. C., Wulder, M. A., & Sanelli, M. (2020). Uncovering spatial and ecological variability in gap size frequency distributions in the Canadian boreal forest. *Scientific Reports*, *10*, 1–12. https://doi.org/10.1038/s41598-020-62878-z

Iglhaut, J., Cabo, C., Puliti, S., Piermattei, L., O'Connor, J., & Rosette, J. (2019). Structure from motion photogrammetry in forestry: A review. *Current Forestry Reports*, *5*, 155–168. https://doi.org/10.1007/s40725-019-00094-3

Jennings, S. B., Brown, N. D., & Sheil, D. (1999). Assessing forest canopies and understorey illumination: Canopy closure, canopy cover, and other measures. *Forestry*, *72*, 59–74. https://doi.org/10.1093/forestry/72.1.59

Joyce, K. E., Anderson, K., & Bartolo, R. E. (2021). Of course, we fly unmanned—We're women. *Drones*, *5*, 2–5. https://doi.org/10.3390/drones5010021

Jucker, T., Asner, G. P., Dalponte, M., Brodrick, P., Christopher, D., Vaughn, N., et al. (2018). Estimating aboveground carbon density and its uncertainty in Borneo's structurally complex tropical forests using airborne laser scanning. *Biogeosciences*, 1–29.

Jucker, T., Asner, G. P., Dalponte, M., Brodrick, P. G., Philipson, C. D., Vaughn, N. R., et al. (2018). Estimating aboveground carbon density and its uncertainty in Borneo's structurally complex tropical forests using airborne laser scanning. *Biogeosciences*, *15*, 3811–3830. https://doi.org/10.5194/bg-15-3811-2018

Jucker, T., Caspersen, J., Chave, J., Antin, C., Barbier, N., Bongers, F., et al. (2017). Allometric equations for integrating remote sensing imagery into forest monitoring programmes. *Global Change Biology*, *23*, 177–190. https://doi.org/10.1111/gcb.13388

Kellner, J. R., Armston, J., Birrer, M., Cushman, K. C., Duncanson, L., Eck, C., et al. (2019). New opportunities for forest remote sensing through ultra-high-density drone LiDAR. *Surveys in Geophysics*, *40*, 959–977. https://doi.org/10.1007/s10712-019-09529-9

Khosravipour, A., Skidmore, A. K., Isenburg, M., Wang, T., & Hussin, Y. A. (2014). Generating pit-free canopy height models from airborne LiDAR. *Photogrammetric Engineering & Remote Sensing*, *80*, 863–872. https://doi.org/10.14358/pers.80.9.863

Knapp, N., Fischer, R., Cazcarra-Bes, V., & Huth, A. (2020). Structure metrics to generalize biomass estimation from LiDAR across forest types from different continents. *Remote Sensing of Environment*, *237*, 111597. https://doi.org/10.1016/j.rse.2019.111597

Krause, S., Sanders, T. G. M., Mund, J. P., & Greve, K. (2019). UAV-based photogrammetric tree height measurement for intensive forest monitoring. *Remote Sensing*, *11*, 1–18. https://doi.org/10.3390/rs11070758

Lopatin, J., Dolos, K., Hernández, H. J., Galleguillos, M., & Fassnacht, F. E. (2016). Comparing generalized linear models and random forest to model vascular plant species richness using LiDAR data in a natural forest in central Chile. *Remote Sensing of Environment*, *173*, 200–210. https://doi.org/10.1016/j.rse.2015.11.029

Marselis, S. M., Abernethy, K., Alonso, A., Armston, J., Baker, T. R., Bastin, J. F., et al. (2020). Evaluating the potential of full-waveform LiDAR for mapping pan-tropical tree species richness. *Global Ecology and Biogeography*, *29*, 1799–1816. https://doi.org/10.1111/geb.13158

Meyer, V., Saatchi, S. S., Chave, J., Dalling, J. W., Bohlman, S., Fricker, G. A., et al. (2013). Detecting tropical forest biomass dynamics from repeated airborne LiDAR measurements. *Biogeosciences*, *10*, 5421–5438. https://doi.org/10.5194/bg-10-5421-2013

Mlambo, R., Woodhouse, I. H., Gerard, F., & Anderson, K. (2017). Structure from motion (SfM) photogrammetry with drone data: A low cost method for monitoring greenhouse gas emissions from forests in developing countries. *Forests*, *8*. https://doi.org/10.3390/f8030068

Puliti, S., Breidenbach, J., & Astrup, R. (2020). Estimation of forest growing stock volume with UAV laser scanning data: Can it be done without field data? *Remote Sensing*, *12*. https://doi.org/10.3390/rs12081245

Puliti, S., Dash, J. P., Watt, M. S., Breidenbach, J., & Pearse, G. D. (2020). A comparison of UAV laser scanning, photogrammetry, and airborne laser scanning for precision inventory of small-forest properties. *Forestry: An International Journal of Forest Research*, *93*, 150–162. https://doi.org/10.1093/forestry/cpz057

Qi, W., Saarela, S., Armston, J., Ståhl, G., & Dubayah, R. (2019). Forest biomass estimation over three distinct forest types using TanDEM-X InSAR data and simulated GEDI LiDAR data. *Remote Sensing of Environment*, *232*, 111283. https://doi.org/10.1016/j.rse.2019.111283

Roșca, S., Suomalainen, J., Bartholomeus, H., & Herold, M. (2018). Comparing terrestrial laser scanning and unmanned aerial vehicle structure from motion to assess top of canopy structure in tropical forests. *Interface Focus*, *8*.

Roussel, J. R., Auty, D., Coops, N. C., Tompalski, P., Goodbody, T. R. H., Meador, A. S., et al. (2020). lidR: An R package for analysis of airborne laser scanning (ALS) data. *Remote Sensing of Environment*, *251*, 112061. https://doi.org/10.1016/j.rse.2020.112061

Schneider, F. D., Ferraz, A., Hancock, S., Duncanson, L. I., Dubayah, R. O., Pavlick, R. P., & Schimel, D. S. (2020). Towards mapping the diversity of canopy structure from space with GEDI. *Environmental Research Letters*, *15*. https://doi.org/10.1088/1748-9326/ab9e99

Schneider, F. D., Morsdorf, F., Schmid, B., Petchey, O. L., Hueni, A., Schimel, D. S., & Schaepman, M. E. (2017). Mapping functional diversity from remotely sensed morphological and physiological forest traits. *Nature Communications*, *8*. https://doi.org/10.1038/s41467-017-01530-3

Silva, C. A., Valbuena, R., Pinagé, E. R., Mohan, M., de Almeida, D. R. A., North Broadbent, E., et al. (2019). ForestGapR: An R Package for forest gap analysis from canopy height models. *Methods in Ecology and Evolution*, *10*, 1347–1356. https://doi.org/10.1111/2041-210x.13211

St-Onge, B., Vega, C., Fournier, R. A., & Hu, Y. (2008). Mapping canopy height using a combination of digital stereo-photogrammetry and LiDAR. *International Journal of Remote Sensing*, *29*, 3343–3364.

Swinfield, T., Lindsell, J. A., Williams, J., Harrison, R. D., Agustiono, H., Gemita, E., et al. (2019). Accurate measurement of tropical forest canopy heights and aboveground carbon using structure from motion. *Remote Sensing*, *11*. https://doi.org/10.3390/rs11080928

Tompalski, P., White, J. C., Coops, N. C., & Wulder, M. A. (2019). Demonstrating the transferability of forest inventory attribute models derived using airborne laser scanning data. *Remote Sensing of Environment*, *227*, 110–124. https://doi.org/10.1016/j.rse.2019.04.006

Vaglio Laurin, G., Ding, J., Disney, M., Bartholomeus, H., Herold, M., Papale, D., & Valentini, R. (2019). Tree height in tropical forest as measured by different ground, proximal, and remote sensing instruments, and impacts on aboveground biomass estimates. *International Journal of Applied Earth Observation and Geoinformation*, *82*, 101899. https://doi.org/10.1016/j.jag.2019.101899

Valbuena, R., O'Connor, B., Zellweger, F., Simonson, W., Vihervaara, P., Maltamo, M., et al. (2020). Standardizing ecosystem morphological traits from 3D information sources. *Trends in Ecology & Evolution*, *35*, 656–667. https://doi.org/10.1016/j.tree.2020.03.006

Wallace, L., Lucieer, A., Malenovskỳ, Z., Turner, D., & Vopěnka, P. (2016). Assessment of forest structure using two UAV techniques: A comparison of airborne laser scanning and structure from motion (SfM) point clouds. *Forests*, *7*, 1–16. https://doi.org/10.3390/f7030062

Westoby, M. J., Brasington, J., Glasser, N. F., Hambrey, M. J., & Reynolds, J. M. (2012). "Structure-from-Motion" photogrammetry: A low-cost, effective tool for geoscience applications. *Geomorphology*, *179*, 300–314. https://doi.org/10.1016/j.geomorph.2012.08.021

White, J. C., Tompalski, P., Coops, N. C., & Wulder, M. A. (2018). Comparison of airborne laser scanning and digital stereo imagery for characterizing forest canopy gaps in coastal temperate rainforests. *Remote Sensing of Environment*, *208*, 1–14. https://doi.org/10.1016/j.rse.2018.02.002

White, J. C., Wulder, M. A., Vastaranta, M., Coops, N. C., Pitt, D., & Woods, M. (2013). The utility of image-based point clouds for forest inventory: A comparison with airborne laser scanning. *Forests*, *4*, 518–536. https://doi.org/10.3390/f4030518

Williams, J., Schonlieb, C. B., Swinfield, T., Lee, J., Cai, X., Qie, L., & Coomes, D. A. (2020). 3D segmentation of trees through a flexible multiclass graph cut algorithm. *IEEE Transactions on Geoscience and Remote Sensing*, *58*, 754–776. https://doi.org/10.1109/tgrs.2019.2940146

Xu, L., Saatchi, S. S., Shapiro, A., Meyer, V., Ferraz, A., Yang, Y., et al. (2017). Spatial distribution of carbon stored in forests of the Democratic Republic of Congo. *Scientific Reports*, *7*, 1–12. https://doi.org/10.1038/s41598-017-15050-z

Yin, D., & Wang, L. (2019). Individual mangrove tree measurement using UAV-based LiDAR data: Possibilities and challenges. *Remote Sensing of Environment*, *223*, 34–49. https://doi.org/10.1016/j.rse.2018.12.034

Zhang, W., Qi, J., Wan, P., Wang, H., Xie, D., Wang, X., & Yan, G. (2016). An easy-to-use airborne LiDAR data filtering method based on cloth simulation. *Remote Sensing*, *8*, 1–22. https://doi.org/10.3390/rs8060501